Cryptates from
1,1″ : 1′,1‴-bis(1,4,10,13-tetraoxa-7,16-diazacyclooctadecane-
7,16-dimethylene) bisferrocene

C. Dennis Hall [a,*], Andreas Leineweber [a], James H.R. Tucker [a], David J. Williams [b]

[a] *Department of Chemistry, King's College London, Strand, London WC2R 2LS, UK*
[b] *Department of Chemistry, Imperial College of Science Technology and Medicine, London SW7 2AY, UK*

Abstract

Complexation of the title compound (6, $n = m = 2$) with a range of cations has been examined in solution by ^1H and ^{13}C NMR spectroscopy and the solid state structure of the binuclear cryptate of 6 with calcium triflate determined by X-ray crystallography. The isolation of a trimer, 1,1″ : 1′,1‴ : 1‴″,1‴″‴-tris(1,4,10,11-tetraoxa-7,16-diazacyclooctadecane-7,16-dicarbonyl)trisferrocene is also reported.

Keywords: Iron; Cryptates; Ferrocene; NMR; Crystal structure; X-ray diffraction

1. Introduction

The synthesis and chemistry of macrocycles and cryptands containing metallocene units has developed substantially over the last fifteen years [1-3]. A common route into these molecular systems involves the condensation of ferrocene bis-acid chloride (1) with diazamacrocycles (2), which produces a mixture of monomeric (3) and dimeric (4) cryptands together with oligomeric species in overall ratios which depend upon the reaction conditions. The monomeric and dimeric compounds may be separated from each other and from the oligomeric species by careful chromatography, and the amide groups of each can be reduced to amines (5 and 6) using the method developed by Gokel and coworkers [4]. Both types of cryptand form complexes with a wide variety of monovalent, divalent or trivalent cations, and in each case the complexes may be characterised by mass spectrometry and a combination of UV–vis, IR and multinuclear NMR spectroscopy. In some cases the structures have been determined by X-ray crystallography, and in every complex derived from non-reduced cryptands the oxygen atoms of the

amide links were involved as ligands [5–8]. X-ray crystal structures of the Na$^+$ and Ag$^+$ complexes of (5, $m = n = 2$), however, revealed that the cations were encapsulated within the macrocyclic cavity and the Fe–Ag$^+$ distance (337 pm) suggested direct interaction between the metal centres [4]. In the case of the reduced dimeric cryptands 6, dinuclear cryptates are possible and two types of structure (7a or 7b) may be envisaged for such complexes. This paper reports the multinuclear NMR data on a series of cryptates from (6, $n = m = 2$) and an X-ray crystal structure of the binuclear cryptate formed with calcium triflate confirms 7b as the correct structure, as recently reported by Plenio and Diodone [9] for the bis-RbI adduct of 6.

2. Experimental

2.1. Instrumentation

^1H and ^{13}C NMR spectra were obtained on either Bruker AM360 or Bruker AM400 spectrometers. Infrared spectra were obtained as KBr pellets on a PE 1600 Series FT-IR spectrometer and mass spectra were recorded on either a Kratos MS890 instrument or a VG 7070 mass spectrometer using the FAB technique with

---

* Corresponding author.

(1)

(2)   m=1-3   ;   n=1-3

Et$_3$N / toluene

(3)

(4)

LiAlH$_4$

LiAlH$_4$

(5)

(6)
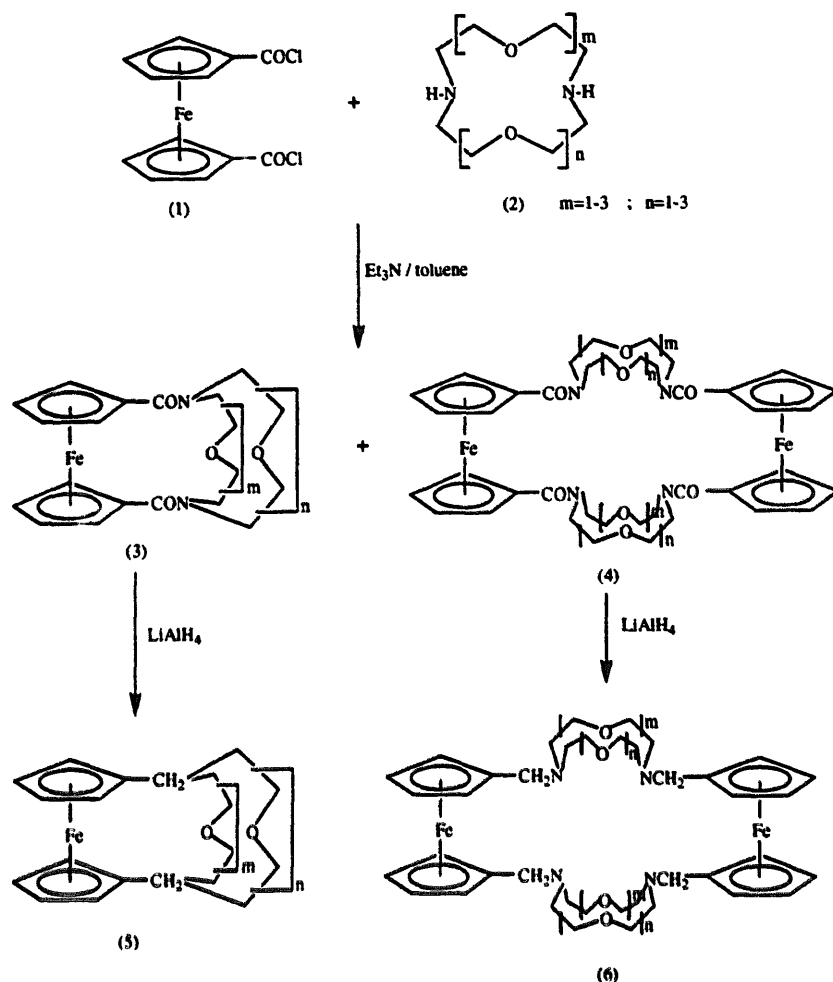
3-NBA as matrix. The crystal structure determination was carried out at Imperial College, London on a Siemens P4 diffractometer (vide infra for crystal data).
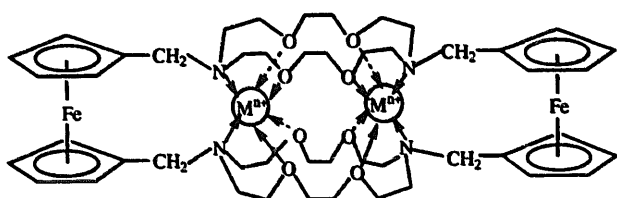
2.2. Preparation of 1,1" : 1',1"'-bis(1,4,10,13-tetraoxa-7,16-diazacyclooctadecane-7,16-dimethylene)bisferrocene (6, m = n = 2)

1,1'-Bis-chlorocarbonylferrocene (1) was prepared from 1,1'-ferrocenedicarboxylic acid by an improved [1] version of the usual reaction with oxalyl chloride. A three-necked creased flask equipped with a mechanical stirrer was flushed with nitrogen then charged with 1 (613 mg, 1.9 mmol) and triethylamine (0.65 ml, 4 mmol) in dry toluene (500 ml). A solution of
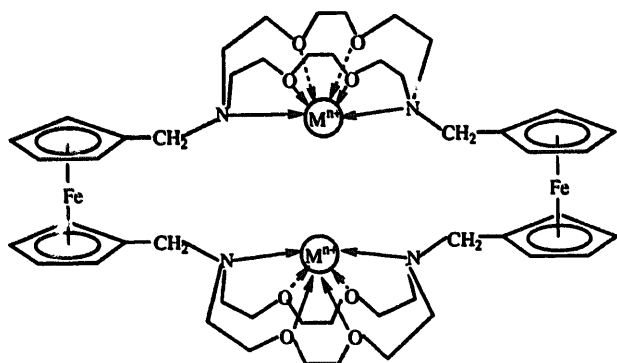

1,4,10,13-tetraoxa-7,16-diazacyclooctadecane (2, n = m = 2, 500 mg, 1.9 mmol) in dry toluene (450 ml) was added dropwise to the vigorously stirred mixture in the flask over 40 min at room temperature. The colour changed from red to orange during the addition and a white precipitate of triethylamine hydrochloride appeared. After stirring overnight the precipitate was filtered off and the filtrate evaporated to leave a crystalline orange residue which was suspended in acetonitrile (25 ml).

The insoluble portion was filtered off, the solid dissolved in the minimum quantity of dichloromethane (ca. 1 ml) and the solution chromatographed on neutral alumina. A yellow band was eluted with 2% (v/v) MeOH in CH$_2$Cl$_2$, which on evaporation yielded 4 (235 mg, 0.24 mmol, 26%), m.p. 244°C, lit. m.p. [3] 243–245°C with IR, ^{1}H and ^{13}C NMR data identical with an authentic sample. The acetonitrile-soluble portion was also chromatographed on neutral alumina and on elution with 0.5% (v/v) MeOH–CH$_2$Cl$_2$ gave 3 (93 mg, 0.19 mmol, 10%), m.p. 183°C, lit. [3] 183–184°C and with 2% (v/v) MeOH–CH$_2$Cl$_2$ gave 96 mg of a material

---

[1] The crude dicarboxylic acid (6.5 g) containing 14% monocarboxylic acid was extracted with diethyl ether (50 ml) in a Soxhlet for 48 h. The procedure left almost pure (> 99.5%, 4.5 g) dicarboxylic acid in the thimble and a mixture of mono (55%) and dicarboxylic acid (45%) in the extract.

(7a)

(7b)

with m.p. > 240°C. A FAB-MS (KRATOS) of the unknown material showed a weak peak at 1501 a.m.u., indicating that the compound was a trimer (8). This conclusion was reinforced by the addition of sodium iodide which produced a peak at 1523 a.m.u. with 80 times the intensity of the parent trimer (vide infra for further discussion of the MS and NMR data). The above preparation was repeated except that the crown ether solution was added over 4 h. This resulted in the isolation of 3 (14%), 4 (20%) and a 1% yield of the trimer 8. When the reaction was repeated by adding the acid chloride to the diazacrown plus triethylamine over 4 h, only a trace of the trimer was detected by TLC [2] and the yields of 3 and 4 were 40% and 22% respectively. Compound 3 was readily reduced to 5 in 68% yield using the method described previously [4,10].

Reduction of 4 to 6 was achieved in an analogous manner, as follows. The dimer (4, 187 mg, 0.19 mmol) was dissolved in a mixed solvent of anhydrous CH_2Cl_2 (20 ml) and anhydrous THF (4 ml). $LiAlH_4$ (50 mg, 1.32 mol) was added and the mixture was stirred for 24 h at room temperaure. The mixture was then diluted with CH_2Cl_2 (20 ml) and quenched with a saturated solution of potassium tartrate (15 ml). The phases were separated and the aqueous layer was extracted with

CH_2Cl_2 (3 × 10 ml). The combined organic layers were washed with water (2 × 15 ml), dried over $MgSO_4$ and evaporated to give crude 6 (173 mg). The crude product was dissolved in the minimum amount of CH_2Cl_2 and chromatographed on neutral Al_2O_3, deactivated with 3% water. Elution with 1–2% (v/v) MeOH in CH_2Cl_2 gave a yellow band ($R_f = 0.2$ with 5% MeOH in CH_2Cl_2 on Al_2O_3), which on evaporation gave 6 (140 mg, 0.15 mmol, 79%), m.p. 103–105°C, lit. [4] m.p. 104–105°C. Crystallisation of the reduced dimer was induced by addition of diethyl ether to the residue from the column chromatography. The IR and NMR data for 6 are reported in Section 3.

2.3. Preparation of the metal triflates

The metal triflates used for complexation were prepared by a general procedure, described as follows for strontium triflate. Trifluoromethane sulphonic acid (5 ml, 57 mmol) was dissolved in acetonitrile (20 ml) and a slight excess of strontium carbonate (7.76 g, 29 mmol) was added to the stirred solution in small portions. The suspension was heated under relux for 1 h and left overnight to settle. The solution was filtered twice through Celite (to remove excess carbonate), the solvent evaporated and the residue dried under high vacuum in a Kugelrohr at 250°C for 6 h to yield strontium triflate (8.15 g, 21 mmol, 72%) as a white crystalline solid which was totally soluble in acetonitrile or water, the latter solution showing a neutral pH.

2.4. NMR studies of the complexation of 6 with various cations

A known quantity (10–25 mg) of 6 was dissolved in $CDCl_3/CD_3CN$ (0.5 ml, 50% v/v) and a 2.5 molar equivalent of each metal triflate was added to each solution. The solutions were then filtered through a cotton wool plug into 5 mm NMR tubes.

Attempts to prepare a solution of the yttrium complex by the above procedure resulted in almost complete protonation of 6, which could not be deprotonated by either solid potassium carbonate or caesium carbonate. Use of 1,4-diazabicyclo-(2.2.2)-octane to remove the protons in the presence of yttrium was successful, but resulted in the formation of a mixture of yttrium complexes whose structure could not be assigned unambiguously (vide infra).

2.5. Preparation of single crystals of 6. $2[Ca(CF_3-SO_3)_2] \cdot 2H_2O \cdot 2CD_3CN \cdot 2CDCl_3$

A loosely-stoppered NMR tube containing a solution of the calcium triflate of 6, prepared as described above, was placed in a measuring cylinder filled with activated molecular sieves and closed by parafilm. After 5 weeks,

---

[2] TLC of the reaction mixtures on Al_2O_3 eluting with 5% (v/v) MeOH in CH_2Cl_2 produced three spots at $R_f = 0.8$ (3), 0.6 (4) and 0.5, the last being the trimeric species.

yellow crystals which extinguished polarised light formed on the sides of the tube as the solvent evaporated. The material was kept in the tube until mounted on the diffractometer.

2.6. Crystal data and structure analysis

For $C_{58}H_{76}D_8Ca_2F_{12}Fe_2N_6O_{22}S_4Cl_6$: $M = 1985.4$, orthorhombic, $Pbca$, $a = 21.411(4)$, $b = 12.482(3)$, $c = 30.658(3)$ Å, $U = 8194(2)$ Å^3, $z = 4$, $D_c = 1.603$ g cm^{-3}, $\mu = 87.5$ cm^{-1}, $F(000) = 4064$. The crystal data were collected on a Siemens P4 diffractometer using Mo Kα radiation ($\lambda = 0.71073$ Å, graphite monochromator) ω-scans, $T = 223(2)$ K, $2° < 2\theta < 50°$, $R_1(wR_2) = 6.39(15.5)\%$ for 7080 independent reflections of which 5006 had $|F_o| > 4\sigma(F_o)$. The structure was solved by direct methods using the SHELXTL 5.0 (beta-version) programme and refined by full-matrix least-squares on F^2. Atomic coordinates are given in Table 1 and selected bond angles and bond lengths in Table 2. Tables of anisotropic thermal parameters and hydrogen atom coordinates and a complete list of bond lengths and angles have been deposited at the Cambridge Crystallographic Data Centre.

3. Results and discussion

3.1. The isolation and characterisation of 1,1″ : 1′,1‴ : 1″″,1″″′-tris(1,4,10,14-tetraoxa-7,16-diaza-cyclooctadecane-7,16-di-carbonyl)trisferrocene (8)

As noted in the Experimental section, addition of the diazacrown to 1 over 40 min with vigorous stirring gave the expected products 3 and 4 in 10% and 26% yields respectively, but a 10% yield of a trimer (8) was also obtained which was characterised by FAB mass spectrometry of the cryptand and its complex with Na$^+$. The latter mass spectrum was much more intense than the FAB spectrum of the cryptand and gave the isotope pattern shown in Fig. 1, which includes the theoretical pattern for comparison. The ^{1}H and ^{13}C NMR spectra of 4 and 8 are very similar (Table 3) but not identical. In particular, the region around δ 3.5–4.0 in the ^{1}H NMR distinguishes the two compounds (Fig. 2). As a further comparison, the amide carbonyl stretching vibrations of 4 and 8 occur at 1621 and 1613 cm^{-1} respectively.

3.2. Complex formation between 6 and metal cations

A sample of the pure dimer 4 was reduced to the tetramine 6 using LiAlH$_4$ in a mixture of CH$_2$Cl$_2$ and

Table 1

Atomic coordinates ($\times 10^4$) and equivalent isotropic displacement parameters (Å$\times 10^3$) for 6. $2Ca(CF_3SO_3)_2 \cdot 2H_2O$

Atom	x	y	z	U_{eq}
Fe	−2433(1)	4905(1)	−323(1)	28(1)
Ca	−326(1)	3954(1)	1250(1)	24(1)
C(1)	−1890(2)	3881(4)	−679(2)	33(1)
C(2)	−2530(2)	3618(4)	−724(2)	38(1)
C(3)	−2839(2)	4517(5)	−905(2)	39(1)
C(4)	−2399(2)	5346(5)	−964(2)	35(1)
C(5)	−1804(2)	4946(4)	−826(1)	31(1)
C(6)	−1178(2)	5509(5)	−838(2)	34(1)
N(7)	−930(2)	5712(4)	−1288(1)	33(1)
C(8)	−986(2)	4722(5)	−1546(2)	39(1)
C(9)	−1247(3)	6636(5)	−1492(2)	46(1)
C(10)	−836(3)	7294(5)	−1783(2)	49(2)
O(11)	−278(2)	7543(3)	−1546(1)	41(1)
C(12)	84(3)	8366(5)	−1752(2)	48(1)
C(13)	590(3)	8664(4)	−1440(2)	46(1)
O(14)	933(2)	7724(3)	−1338(1)	35(1)
C(15)	1415(3)	7911(4)	−1019(2)	40(1)
C(16)	−2134(2)	5916(4)	158(2)	32(1)
C(17)	−2755(3)	6176(5)	35(2)	38(1)
C(18)	−3131(2)	5263(5)	109(2)	39(1)
C(19)	−2742(2)	4434(4)	273(2)	34(1)
C(20)	−2119(2)	4830(4)	305(1)	28(1)
C(21)	−1539(2)	4268(4)	468(1)	29(1)
N(22)	−1532(2)	4037(3)	946(1)	28(1)
C(23)	−1855(2)	3019(4)	1038(2)	38(1)
C(24)	−1803(2)	4940(4)	1190(2)	34(1)
C(25)	−1734(2)	4815(5)	1681(2)	41(1)
O(26)	−1094(2)	4604(3)	1763(1)	41(1)
C(27)	−936(3)	4469(5)	2212(2)	43(1)
C(28)	−337(2)	5036(5)	2289(2)	41(1)
O(29)	65(2)	4769(3)	1931(1)	38(1)
C(30)	674(3)	5224(5)	1984(2)	47(2)
O(31)	−315(2)	5696(3)	982(1)	37(1)
S(40)	−30(1)	2946(1)	110(1)	36(1)
O(41)	−582(2)	2666(5)	−118(2)	76(2)
O(42)	−125(2)	3265(3)	557(1)	39(1)
O(43)	402(2)	3614(4)	−122(1)	62(1)
C(44)	395(3)	1698(5)	167(2)	56(2)
F(45)	76(3)	981(4)	375(2)	120(2)
F(46)	921(2)	1836(4)	374(2)	104(2)
F(47)	525(2)	1288(4)	−221(1)	87(1)
S(50)	−4146(1)	2966(1)	1817(1)	43(1)
O(51)	−4375(3)	3934(4)	1985(2)	78(2)
O(52)	−3727(3)	2403(5)	2094(2)	110(2)
O(53)	−4595(2)	2282(3)	1609(1)	58(1)
C(54)	−3660(4)	3416(6)	1369(3)	69(2)
F(55)	−3231(2)	4076(4)	1507(2)	106(2)
F(56)	−3991(3)	3949(4)	1076(2)	116(2)
F(57)	−3395(3)	2613(4)	1172(2)	155(3)
C(60)	−2459(3)	1953(7)	2592(2)	68(2)
Cl(61)	−2122(2)	2965(3)	2875(1)	170(2)
Cl(62)	−1917(1)	1494(3)	2205(1)	116(1)
Cl(63)	−2698(1)	963(2)	2932(1)	110(1)
C(70)	−722(5)	11485(8)	−1022(3)	101(3)
C(71)	−906(3)	10945(6)	−1409(2)	65(2)
N(72)	−1030(4)	10432(7)	−1702(2)	95(2)

U_{eq} is defined as one third of the trace of the orthogonalized U_{ij} tensor.

THF, and the progress of the reduction was monitored by TLC on Al_2O_3 plates. The IR data on the isolated product indicated the presence of water of crystallisation and the ^1H and ^{13}C NMR data of 6 are shown in Table 4. Complexation of 6 with a wide range of cationic triflates was then studied by ^1H and ^{13}C NMR, and the relevant data are also shown in Table 4. All the complexes showed 2:1 (cation:ligand) stoichiometry,

and major changes in the ^1H NMR spectra were observed for the N-methylene protons (labelled 3) attached to the cyclopentadiene rings. Within any one series of monovalent (Na^+, K^+, Cs^+) or divalent (Ca^{2+}, Sr^{2+}, Ba^{2+}) cations, these protons moved downfield to extents which correlated with the charge densities of each set of cations. Protonation (by addition of $4 \times H^+$) generated a very large shift to 4.55 ppm, consistent with

Table 2

Selected bond lengths (Å) and angles (deg) for 6. $2Ca(CF_3SO_3)_2 \cdot 2H_2O$

Ca-O(31)	2.325(3)	Ca-O(42)	2.333(3)
Ca-O(26)	2.413(3)	Ca-O(11)#1	2.449(4)
Ca-O(29)	2.469(3)	Ca-O(14)#1	2.479(3)
Ca-N(7)#1	2.726(4)	Ca-N(22)	2.747(4)
C(6)-N(7)	1.498(6)	N(7)-C(8)	1.473(7)
N(7)-C(9)	1.477(7)	N(7)-Ca#1	2.726(4)
C(8)-C(30)#1	1.503(7)	C(9)-C(10)	1.498(8)
C(10)-O(11)	1.431(6)	O(11)-C(12)	1.433(6)
O(11)-Ca#1	2.449(4)	C(12)-C(13)	1.493(8)
C(13)-O(14)	1.418(6)	O(14)-C(15)	1.442(6)
O(14)-Ca#1	2.479(3)	C(15)-C(23)#1	1.496(8)
C(21)-N(22)	1.492(5)	N(22)-C(24)	1.473(6)
N(22)-C(23)	1.474(6)	C(23)-C(15)#1	1.496(8)
C(24)-C(25)	1.521(6)	C(25)-O(26)	1.416(6)
O(26)-C(27)	1.430(6)	C(27)-C(28)	1.483(8)
C(28)-O(29)	1.432(6)	O(29)-C(30)	1.432(6)
C(30)-C(8)#1	1.503(7)		
O(31)-Ca-O(26)	85.60(13)	O(31)-Ca-O(42)	91.19(13)
O(31)-Ca-O(11)#1	147.09(13)	O(42)-Ca-O(26)	147.42(12)
O(26)-Ca-O(11)#1	112.04(13)	O(42)-Ca-O(11)#1	87.62(13)
O(42)-Ca-O(29)	149.26(12)	O(31)-Ca-O(29)	84.84(13)
O(11)#1-Ca-O(29)	79.71(13)	O(26)-Ca-O(29)	62.77(11)
O(42)-Ca-O(14)#1	83.35(13)	O(31)-Ca-O(14)#1	146.56(12)
O(11)#1-Ca-O(14)#1	65.88(12)	O(26)-Ca-O(14)#1	81.75(13)
O(31)-Ca-N(7)#1	82.03(13)	O(29)-Ca-O(14)#1	115.71(12)
O(26)-Ca-N(7)#1	126.42(12)	O(42)-Ca-N(7)#1	84.95(12)
O(29)-Ca-N(7)#1	64.31(11)	O(11)#1-Ca-N(7)#1	65.09(13)
O(31)-Ca-N(22)	81.66(12)	O(14)#1-Ca-N(7)#1	129.89(13)
O(26)-Ca-N(22)	64.44(11)	O(42)-Ca-N(22)	83.00(12)
O(29)-Ca-N(22)	126.21(12)	O(11)#1-Ca-N(22)	130.66(13)
N(7)#1-Ca-N(22)	159.47(12)	O(14)#1-Ca-N(22)	64.95(12)
C(8)-N(7)-C(9)	112.9(4)	N(7)-C(6)-C(5)	114.6(4)
C(9)-N(7)-C(6)	111.1(4)	C(8)-N(7)-C(6)	108.9(4)
C(9)-N(7)-Ca#1	110.6(3)	C(8)-N(7)-Ca#1	103.3(3)
N(7)-C(8)-C(30)#1	114.0(5)	C(6)-N(7)-Ca#1	109.7(3)
O(11)-C(10)-C(9)	108.0(4)	N(7)-C(9)-C(10)	114.2(4)
C(10)-O(11)-Ca#1	117.6(3)	C(10)-O(11)-C(12)	112.6(4)
O(11)-C(12)-C(13)	106.8(4)	C(12)-O(11)-Ca#1	115.1(3)
C(13)-O(14)-C(15)	112.6(4)	O(14)-C(13)-C(12)	108.0(4)
C(15)-O(14)-Ca#1	116.0(3)	C(13)-O(14)-Ca#1	116.9(3)
N(22)-C(21)-C(20)	115.0(4)	O(14)-C(15)-C(23)#1	107.3(4)
C(24)-N(22)-C(21)	110.3(4)	C(24)-N(22)-C(23)	112.2(4)
C(24)-N(22)-Ca	103.1(3)	C(23)-N(22)-C(21)	110.5(4)
C(21)-N(22)-Ca	110.5(3)	C(23)-N(22)-Ca	110.1(3)
N(22)-C(24)-C(25)	112.7(4)	N(22)-C(23)-C(15)#1	111.5(4)
C(25)-O(26)-C(27)	114.9(4)	O(26)-C(25)-C(24)	106.7(4)
C(27)-O(26)-Ca	115.3(3)	C(25)-O(26)-Ca	127.3(3)
O(29)-C(28)-C(27)	106.7(4)	O(26)-C(27)-C(28)	107.5(4)
C(30)-O(29)-Ca	124.7(3)	C(30)-O(29)-C(28)	111.6(4)
O(29)-C(30)-C(8)#1	108.7(4)	C(28)-O(29)-Ca	122.6(3)

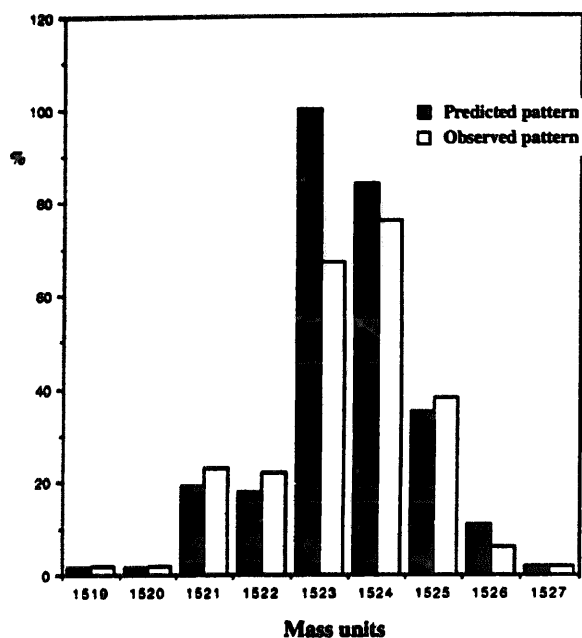Symmetry transformations used to generate equivalent atoms: #1 $-x$, $-y+1$, $-z$.

Compound 4			Compound 8		
δ(ppm)	Int.	Assign-ment	δ (ppm)	Int.	Assign-ment
^{1}H NMR					
4.62(br)	4H	1	4.64t	4H	1
4.34(br)	4H	2	4.38t	4H	2
3.6–4.0	24H	3a–5b	3.55–3.90	24H	3a–5b
^{13}C NMR					
170.1	0	d	170.1	0	d
79.4	0	a	79.8	0	a
73.9	+	b	72.2	+	b
72.0	−	f/g	71.5	+	c
70.3	−	c/f/g	70.7	−	f/g
70.1	−	c/f/g	69.7	−	f/g
49.3	−	e	49.5	−	e
47.3	−	e′	47.6	−	e′

Fig. 1. Comparison of the observed (□) isotope pattern with the predicted (■) for the complex between 8 and Na⁺.

these findings. The multiplet structure, relative shifts and integration values made the assignment of the ^{1}H NMR signals quite straightforward, but carbon atoms

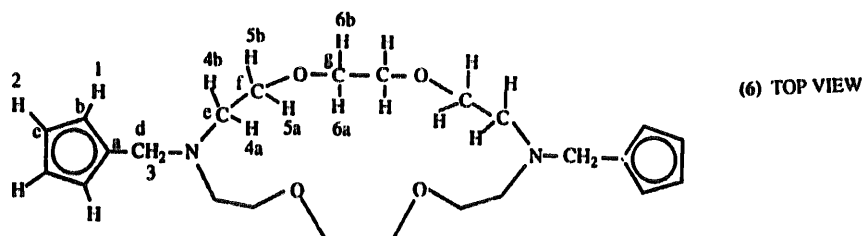Compound (4)

Compound (8)
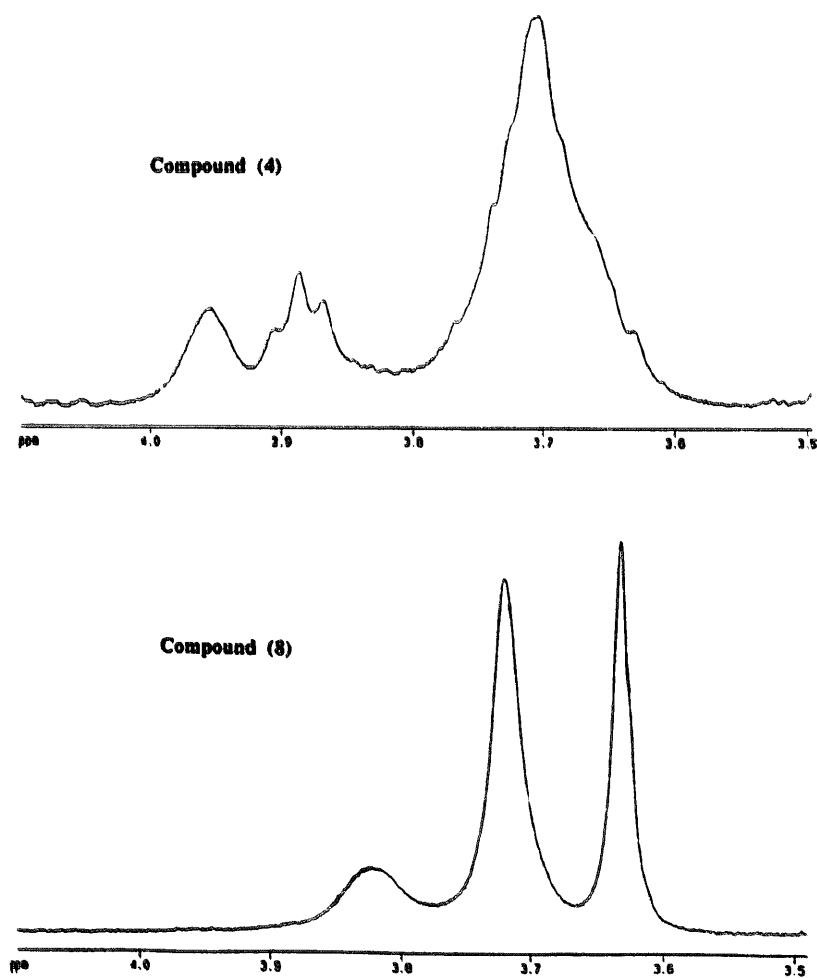
Fig. 2. Comparison of the expanded ^{1}H NMR spectra at δ 3.5–4.0 for 4 and 8.

b/c and f/g could not be distinguished except in the protonated species in which the assignment was accomplished through heteronuclear $^1H/^{13}C$ correlation data. A signal due to carbon atom a could not be found in the spectrum of the caesium complex, probably because it was hidden beneath the $CDCl_3$ triplet. The NCH_2 carbon atoms (d and e) were initially distinguished by the intensities of the signals e > d, but since this criterion was somewhat dubious, the assignment was confirmed for the calcium complex by NOE on the singlet at δ = 53.1 ppm on irradiation of the protons at 3.93 ppm. As mentioned above, a complete assignment for the protonated cryptand was achieved by homo- and heteronuclear correlation spectra. With the exception of protons 4a and 4b, the signals of the ^1H NMR spectra generally exhibit downfield shifts on complexation. The effect is presumably due to withdrawal of electron density and is more pronounced for smaller, highly charged cations and most marked in the chemical shifts of proton 3. The signals of protons 4a and 4b are

strongly separated by complexation with smaller cations (e.g. Na^+ or Ca^+) with one signal moving upfield by 0.3–0.4 ppm. With larger cations (e.g. K^+, Cs^+, Sr^{2+}, Ba^{2+}) the separation is much less and sometimes unobservable, but the shifts are generally upfield of the parent macrocycle, a phenomenon which is probably ascribed to conformational changes consequent on complexation. The protonated dimer, however, offers a distinct difference with protons 4a and 4b separating and being shifted downfield by 0.56–0.68 ppm. The proton signals of the cyclopentadiene rings are barely changed by complexation except by protonation, where downfield shifts of ca. 0.4 ppm are again observed. The slight downfield shifts of carbon atoms b and c which occur on complexation are more pronounced with the smaller cations in each mono- or divalent series, and again the effect is most pronounced on protonation. The signal of carbon a, however, moves upfield on complexation with the shift for Ca^{2+} being greater than for the similarly sized Na^+, but the effect of protonation again being

Table 4
^1H and ^{13}C NMR data of 6 and its complexes with a variety of monovalent and divalent cations

^1H NMR

Assignment	Integration	Uncomplexed δ (ppm)	+2Na$^+$ δ (ppm)	+2K$^+$ δ (ppm)	+2CS^{+a} δ (ppm)	+2Ca^{2+} δ (ppm)	+2Sr^{2+} δ (ppm)	+2Ba^{2+} δ (ppm)	+4H$^+$ δ (ppm)
1/2	8H	4.11 t	4.18	4.15 t	4.16 t	4.20 m	4.18 t	4.18	4.53
1/2	8H	4.08 t	4.12	4.05 t	4.06 t	4.14 m	4.06 t	4.08	4.49
3	8H	3.62 m	3.82	3.74 s	3.61 s	3.93 s	3.90 s	3.86	4.55
6a + b	16H		3.42	3.56 m	3.55 br	3.78 s	3.77 s	3.75	3.62
5a/b	8H	3.58 t				3.8 m	3.66 m	3.61 s	
5a/b	8H			3.42 t	3.40 br	3.65 m			3.75
4a/b	8H	2.69 t	2.79 s	2.50 m	2.45 br	2.83 m	2.53 m	2.55 m	3.37
4a/b	8H		2.39 d	2.39 m	2.35 br	2.41 dt			3.25
R_3N^+-H	4H								7.7 ^{b}

^{13}C NMR

Assignment	DEPT	Uncomplexed δ (ppm)	+2Na$^+$ δ (ppm)	+2K$^+$ δ (ppm)	+2Cs$^+$ δ (ppm)	2Ca^{2+} δ (ppm)	+2Sr^{2+} δ (ppm)	+2Ba^{2+} δ (ppm)	+4H$^+$ δ (ppm)
a	0	83.1	82.8	80.6	—	80.0	77.8	78.4	74.2
b/c	+	71.0	71.9	71.2	71.0	72.0	71.0	71.1	73.6
b/c	+	68.5	69.0	68.9	68.8	69.4	69.1	69.1	71.8
f/g	−	70.7	68.9	70.7	71.2	69.9	70.2	70.9	70.6 (g)
f/g	−	69.2	67.9	68.0	68.4	69.0	67.8	68.3	64.3 (f)
d	−	53.3	54.9	51.1	50.9	53.2	49.6	49.6	55.3
e	−	53.6	52.4	52.2	52.3	50.4	51.3	52.3	53.1

(6) TOP VIEW

^{a} Low temperature ^1H NMR measurements (to −40°C) gave improved signal resolution, confirming that the broad peaks are due to fluxionality on the time-scale of the experiment; the 6a- and 6b-protons appear to become unequivalent at low temperature.
^{b} Broad peak δ is variable between 7.6 and 7.8.

most pronounced with a shift of 9 ppm. The explanation lies in the electric field effect [11] on the carbon atom α to the protonated (or complexed) nitrogen which overides the inductive effect on the β-carbon. A smaller upfield shift of carbon 4 in the protonated compound is also observed, but uncertain assignment of carbons f and g in both complexed and uncomplexed 6, together with conformational effects, makes a sensible discussion of the shifts of carbons d–g difficult. In summary, although complexation brings about changes in the chemical shifts, the systematic eight-fold (D_{2h}) symmetry of 6 remains intact on complexation or protonation, and this indicates a highly symmetrical structure for the binuclear complexes of 6 in solution.

An attempt to prepare the yttrium complex of 6 in solution by using intensely dried (150°C, 0.1 mm) $Y^{3+}(CF_3SO_3^-)_3$ and deuterated solvents dried over molecular sieves was unsuccessful, since the ^{1}H NMR spectrum was largely that of the protonated complex. Addition of 1,1-diaza-bicyclo-(2.2.2)-octane to deprotonate 6 gave ambiguous results. At least two isomeric Y^{3+} complex species were observed, both of which showed signal patterns analogous to other complexes, but the results were not reproducible.

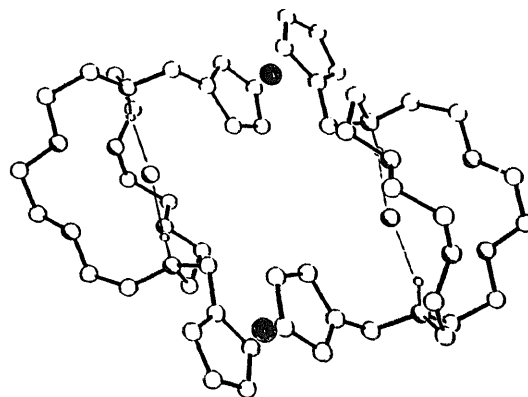Fig. 3. X-ray crystal structure of 6: $2HClO_4 \cdot 2H_2O$.

3.3. Crystal structure of 6. $2Ca(CF_3SO_3)_2 \cdot 2H_2O$

During previous investigations by Tucker [12] a single crystal of 6: $2HClO_4 \cdot 2H_2O$ was obtained and examined by X-ray diffraction. The data suggested that the protonated amine groups were hydrogen-bonded to two water molecules located inside each crown unit (Fig. 3), but the refinement of the structure was poor
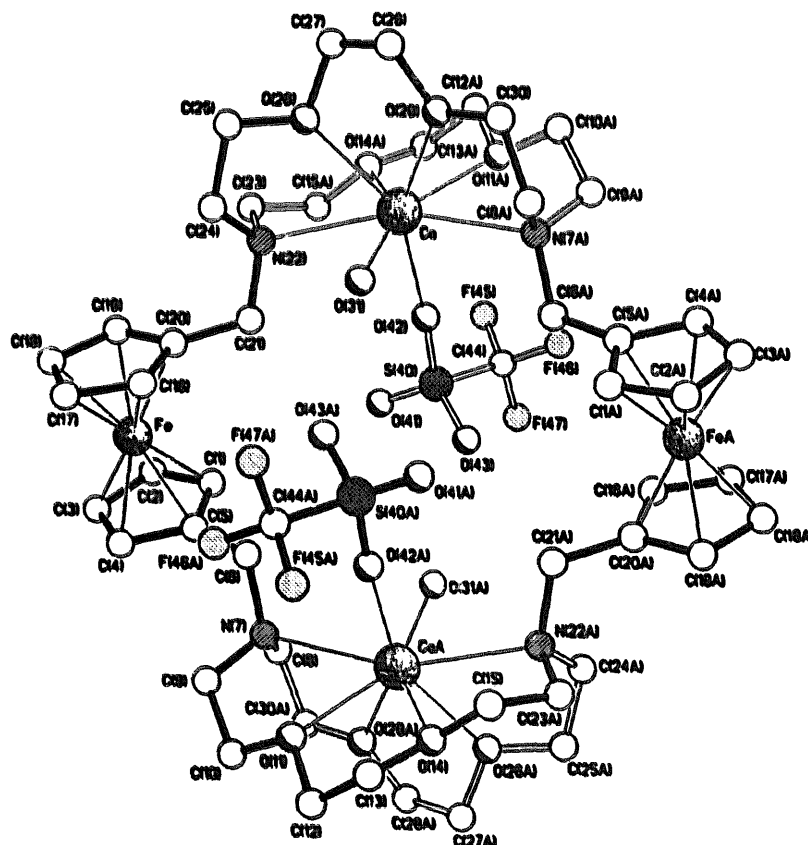

Fig. 4. General view of the complex between 6 and $2Ca^{2+}(CF_3SO_3^-)_4$ along the 011-direction; additional ligands at each octacoordinate calcium ion correspond to a molecule of water and to an oxygen atom (coordinated) of a triflate ion.
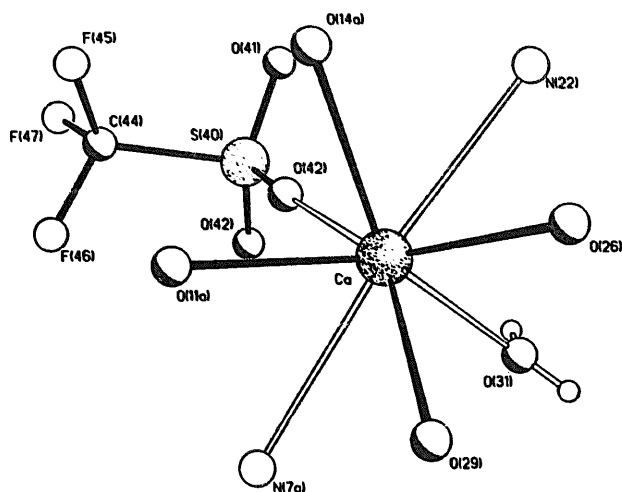
Fig. 5. Coordination sphere of each calcium ion composed of 2×N and 4×O atoms from a diazacrown unit, one triflate ion and one molecule of water.

Fig. 6. The complex of 6 with 2Ca^{2+} viewed along the z-axis with coordinating water molecules within the cavity shown but coordinating triflate ions omitted.

and there was a high degree of disorder in the polyether chains and the perchlorate anions.

Crystals were grown from a CDCl$_3$/CD$_3$CN solution of the complex between calcium triflate and **6**, but were found to decompose on contact with air for several hours, crumbling into layers which suggested the loss of solvent molecules. Successful data collection was achieved, however, by coating a crystal with epoxy glue and collecting the data at −50°C.

All atoms occupied the general positions within an orthorhombic cell (space group *Pbca*, No. 61) with the four molecules inside the unit cell having internal C$_i$ symmetry and with the atoms arranged around the Wykoff position 4(b) (0, 0, $\frac{1}{2}$) [13]. The two calcium ions were found within the two macrocyclic cavities which formed a bowl around each calcium ion (Fig. 4). The eight-fold coordination around each Ca^{2+} is made up of the two nitrogen and four oxygen atoms of each macrocycle plus one water molecule and the oxygen atom of a triflate anion (Fig. 5).

The solid state structure illustrates the high degree of flexibility of the molecule. The cyclopentadiene rings, being virtually parallel, have an approximately eclipsed conformation with the two substituents rotated by 59.6° relative to each other (Fig. 6). This affords a distance of 1070 pm between the iron atoms and a large distance (822 pm) between the two Ca^{2+} ions, which minimises electrostatic repulsion and leaves enough space for two additional ligands to be attached to the cations.

A recent publication by Plenio and Diodone [9] describes the X-ray crystal structure of the bis-rubidium complex of **6** which (as the iodide) has an Rb–Rb distance of 546 pm with the Rb$^+$ ions just above the "bowl" of the diazacrown cavity and a correspondingly larger Fe–Fe distance of 1274 pm. The overall structure, however, is very similar to that of the calcium
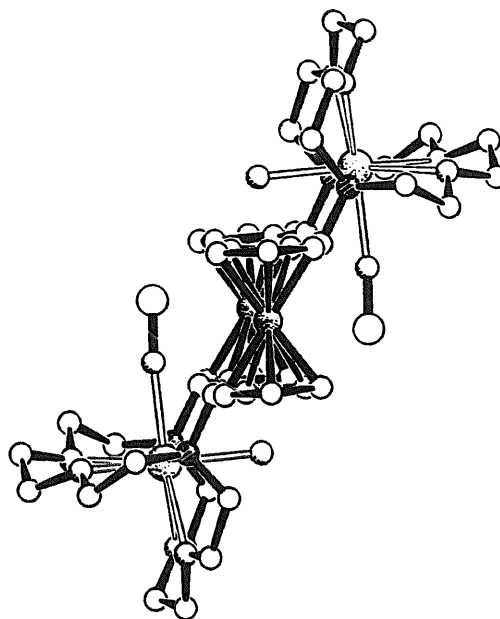
complex and to that of the disodium complex (as the bis-tosylate) of 1,1″ : 1′,1‴-bis(1,4,10-trioxa-7,13-diazacyclopentadecane-7,13-dimethylene)bisferrocene, the reduced 2:1 dimer, which has Na–Na = 701.9 pm and Fe–Fe = 1094 pm.

In addition to the exact two-fold inversion symmetry, the complex exhibits an approximate C$_{2h}$ symmetry (Fig. 7). The higher (eight-fold, D$_{2h}$) symmetry observed in the NMR experiments indicates either a more
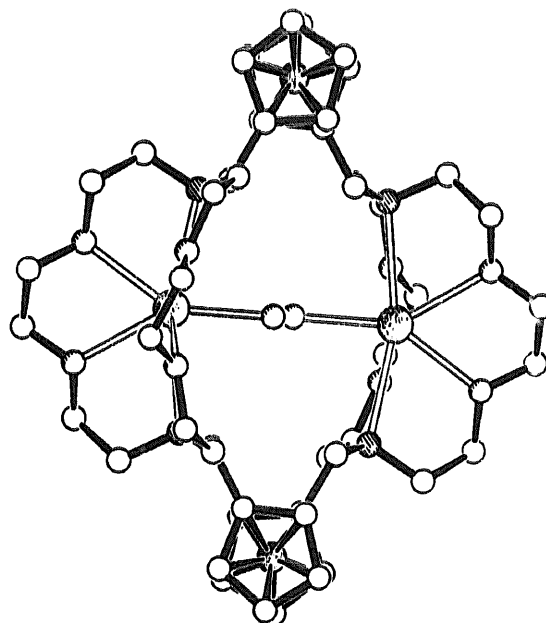

Fig. 7. The complex between 6 and 2Ca^{2+} viewed along the x-axis showing the approximate C$_{2h}$ symmetry in the solid state.

Table 5
Fe–M^{n+} distances (pm) and corresponding $\Delta E_{1/2}$ values (mV) for complexes of 5 and 6 with various cations

Cation (M^{n+})	Cryptand			
	5		6	
	Fe–M^{n+} (pm)	$\Delta E_{1/2}$ (mV)	Fe–M^{n+} (pm)	$\Delta E_{1/2}$ (mV)
Na$^+$	439 [a]	195 [b]	[d]	77 [b]
K$^+$	—	120 [b]	—	38 [b]
Ca^{2+}	366 [c]	291 [b]	671 [e]	164 [b]

[a] Ref. [4]. [b] Ref. [14]. [c] Ref. [9]. [d] It should be noted that the corresponding distance in the Na$^+$: reduced 2:1 dimer complex is 642 pm [9] with $\Delta E_{1/2} = 72$ mV [14]. [e] This work.

symmetrical conformation in solution or, more likely, a rapid interchange of conformations on the NMR time-scale.

The large distance between the Ca^{2+} ions and the Fe atom (both symmetry inequivalent distances of 671 pm) compares with a distance of 675 pm for the Rb$^+$ complex. This explains the smaller anodic shifts on complexation of 6 with cations compared with the $\Delta E_{1/2}$ values observed for 5 where the cation is frequently encapsulated, leading to Fe–Na$^+$ [4] and Fe–Ca^{2+} [9] distances of 439 and 366 pm respectively (Table 5).

In conclusion, the data suggest that there is an inverse relationship between the magnitude of the anodic shifts brought about by cation complexation and the distance between the complexed cation and the redox-active ferrocene centre. More data will be needed to confirm this suggestion, but it is pertinent to note that we have already reported a correlation between $\Delta E_{1/2}$ for complexes of 5 and 6 with charge density $\alpha(c/r^2)$ of the cations used [14]. Since the limited X-ray data indicate Fe=M^{n+} distances d which vary with M^{n+}, it seems reasonable to assume that d will also vary in solution. This in turn implies that the magnitude of d in solution is also linearly related to the charge density of the cation.

Acknowledgements

References

[1] (a) P.D. Beer, Adv. Inorg. Chem., 39 (1992) 79. (b) C.D. Hall, Ferrocenes. From Homogeneous Catalysts to Material Science, in A. Togni and T. Hayashi (eds.) VCH, 1994, pp. 279–316.

[2] (a) F. Vögtle and G. Oepen, Liebigs Ann. Chem., (1979) 1094. (b) A.P. Bell and C.D. Hall, J. Chem. Soc., Chem. Commun., (1980) 163.

[3] A.P. Bell, P.J. Hammond and C.D. Hall, J. Chem. Soc., Perkin Trans. I, (1983) 707.

[4] J.C. Medina, T.T. Goodnow, M.J. Rojas, J.L. Atwood, B.C. Lynn, A.G. Kaifer and G.W. Gokel, J. Am. Chem. Soc., 114 (1992) 10583.

[5] C.D. Hall, J.H.R. Tucker and N.W. Sharpe, Organometallics, 10 (1991) 1727.

[6] C.D. Hall, J.H.R. Tucker, S.Y.F. Chu, A.W. Parkins and S.C. Nyburg, J. Chem. Soc., Chem. Commun., (1993) 1505.

[7] C.D. Hall, J.H.R. Tucker, S.Y.F. Chu and D.J. Williams, J. Chem. Soc. Dalton Trans., (1992) 3133.

[8] C.D. Hall, J.H.R. Tucker and S.Y.F. Chu, J. Organomet. Chem., 448 (1993) 175.

[9] H. Plenio and R. Diodone, J. Organomet. Chem., 492 (1995) 73.

[10] J.C. Medina, T.T. Goodnow, S. Bott, J.L. Atwood, A.E. Kaifer and G.W. Gokel, J. Chem. Soc., Chem. Commun., (1991) 290.

[11] F.W. Wehrly and T. Wirthlin, Interpretation of Carbon-13 NMR Spectra, Heyden, London, 1978, p. 29.

[12] J.H.R. Tucker, PhD Thesis, University of London, 1993.

[13] D.J. Cromer and J.T. Waber, International Tables for X-ray Crystallography, Kynoch Press, Birmingham, UK, 1974.

[14] C.D. Hall and S.Y.F. Chu, J. Organomet. Chem., 498 (1995) 221.